

Multi-site photometric campaign on the high amplitude δ Scuti star KIC 6382916

C. Ulusoy^{1,2}, B. Ulaş³, T. Gülmez¹, L. A. Balona⁴, I. Stateva⁵, I. Kh. Iliev⁵,
D. Dimitrov⁵, H. A. Kobulnicky⁶, T. E. Pickering^{4,7}, L. Fox Machado⁸,
M. Álvarez⁸, R. Michel⁸, K. Antoniuk⁹, D. N. Shakhovskoy⁹, N. Pit⁹,
M. Damasso^{10,11}, D. Cenadelli¹¹, A. Carbognani¹¹

¹Department of Physics, University of Johannesburg, P.O. Box 524, APK Campus, 2006, Johannesburg, South Africa

²Department of Physics, Izmir Institute of Technology, 35430, Izmir, Turkey

³Department of Astronomy and Space Sciences, University of Ege, 35100, Bornova, Izmir, Turkey

⁴South African Astronomical Observatory, P.O. Box 9, Observatory 7935, Cape Town, South Africa

⁵Institute of Astronomy with NAO, Bulgarian Academy of Sciences, blvd. Tsarigradsko chaussee 72, Sofia 1784, Bulgaria

⁶Department of Physics & Astronomy, University of Wyoming, Laramie, WY, 82071, USA

⁷Southern African Large Telescope Foundation, P.O. Box 9, 7935 Observatory, Cape Town, South Africa

⁸Observatorio Astronómico Nacional, Instituto de Astronomía, Universidad Nacional Autónoma de México, Apartado Postal 877, 22830, Ensenada, B.C., México

⁹Crimean Astrophysical Observatory, Scientific Research Institute, 98409, Nauchny, Crimea, Ukraine

¹⁰Astronomical Observatory of the Autonomous Region of the Aosta Valley (OAVdA) Loc. Lignan 39, 11020 Nus (Aosta), Italy

¹¹Department of Physics and Astronomy, University of Padova, vicolo dell'Osservatorio 3, I-35122 Padova, Italy

... Received ...

ABSTRACT

We present results of a multi-site photometric campaign on the high-amplitude δ Scuti star KIC 6382916 in the *Kepler* field. The star was observed over a 85-d interval at five different sites in North America and Europe during 2011. *Kepler* photometry and ground-based multicolour light curves of KIC 6382916 are used to investigate the pulsational content and to identify the principal modes. High-dispersion spectroscopy was also obtained in order to derive the stellar parameters and projected rotational velocity. From an analysis of the *Kepler* time series, three independent frequencies and a few hundred combination frequencies are found. The light curve is dominated by two modes with frequencies $f_1 = 4.9107$ and $f_2 = 6.4314 \text{ d}^{-1}$. The third mode with $f_3 = 8.0350 \text{ d}^{-1}$ has a much lower amplitude. We attempt mode identification by examining the amplitude ratios and phase differences in different wavebands from multicolour photometry and comparing them to calculations for different spherical harmonic degree, l . We find that the theoretical models for f_1 and f_2 are in a best agreement with the observations and lead to value of $l = 1$ modes, but the mode identification of f_3 is uncertain due to its low amplitude. Non-adiabatic pulsation models show that frequencies below 6 d^{-1} are stable, which means that the low frequency of f_1 cannot be reproduced. This is further confirmation that current models predict a narrower pulsation frequency range than actually observed.

Key words: stars: individual: KIC 6382916 - stars: oscillations - stars: variables: δ Scuti

1 INTRODUCTION

The high-amplitude δ Sct (HADS) stars are defined as a Population I subgroup of δ Sct type variables. They are located in the central part of the instability strip (McNamara 2000) in the core or shell hydrogen burning stage of stel-

lar evolution and appear to be intermediate between normal δ Scuti stars and classical Cepheids. However, the distinction between HADS and other δ Sct stars is still rather arbitrary (Soszynski et al. 2008). Their large amplitude, which typically exceeds 0.3 mag, and the presence of many combination

frequencies caused by nonlinear coupling between the principal modes are the defining characteristics (Breger et al. 1998). In general, the HADS appear to pulsate mostly in the fundamental and first overtone radial modes (Balona et al. 2012). However, they need not to be purely radial pulsators, since recent studies have shown that some high-amplitude modes are nonradial (McNamara 2000; Poretti 2003; Poretti et al. 2011).

KIC 6382916 (ASAS 194803+4146.9, $V = 10.79$) was first monitored during the ASAS-3 North station observations and reported as a double-mode HADS star with a period ratio $P_1/P_0 = 0.763$ by Pigulski et al. (2009). The star has also been observed by the *Kepler* satellite in short-cadence (SC, 1-min exposures) and long-cadence (LC, 30-min exposures) modes (Gilliland et al. 2010; Jenkins et al. 2010). The *Kepler* observations are very important as they allow us to fix the frequencies with great precision. We can use these frequencies to fit the multicolour ground-based observations and to determine the amplitudes and phases for the purpose of mode identification.

In this paper, we present results of a multi-site photometric and spectroscopic campaign on the HADS star KIC 6382916 in order to identify the modes of pulsation. Mode identification is the first step in using the frequencies to determine the stellar parameters (asteroseismology). The paper is structured as follows: we first present a detailed description of the ground- and space-based observations including method of data reduction and frequency analyses. Mode identification, which is the main purpose of this study, is presented in Section 6. Finally, we discuss these results.

2 SPECTROSCOPY

Spectroscopic observations were obtained at two different sites. The first set of spectra were obtained with the 2-m RCC telescope of the Bulgarian National Astronomical Observatory, Rozhen. We observed the star during two nights (2011 July 8 and 9) and in three spectral regions 4800–4910 Å ($H\beta$), 4500–4610 Å (Si lines) and 6390–6500 Å (Fe lines). A Photometrics AT200 camera with a SITe SI003AB 1024 × 1024 CCD chip (24 μm pixel size) was used in the third camera of the Coudé spectrograph to provide spectra with a typical resolution of $R = 32\,000$ and a signal-to-noise (S/N) ratio of about 50. The exposure times were 1800 s. The intrinsic spectral line profile, which halfwidth gave about 9 km s^{-1} near 6500 Å, was determined from the arc spectrum. Standard IRAF procedures were used for bias subtraction, flat-fielding and wavelength calibration.

We also obtained spectra of KIC 6382916 using the WIRO longslit spectrograph with an E2V 2048 × 2048 CCD as detector. An 1800 l mm⁻¹ grating in first order yielded a spectral resolution of 1.5 Å near 5800 Å with a $1.2'' \times 100''$ slit. The spectral coverage was 5250–6750 Å. Individual exposure times were 600 s. Reductions followed standard longslit techniques. Each spectrum was shifted by a small amount in velocity so that the Na I D $\lambda\lambda$ 5890, 5996 lines were registered with the mean Na I line wavelength across the ensemble of observations. This zero-point correction to each observation is needed to account for the effects of image wander in the dispersion direction when the stellar FWHM of the point spread function is appreciably less than the slit

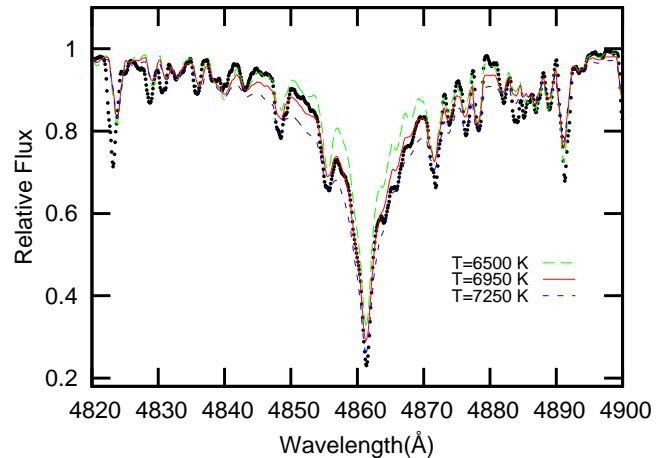


Figure 1. $H\beta$ line (dots) fitted with a model with $T_{\text{eff}} = 6950\text{ K}$, $\log g = 3.7$ (cgs) (solid line). Two other models - $T_{\text{eff}} = 6500\text{ K}$ (long-dashed line) and $T_{\text{eff}} = 7250\text{ K}$ (dashed line) are given for comparison.

width. Multiple exposures were then combined, yielding a final S/N ratio typically in excess of 60 near 5800 Å.

3 ATMOSPHERIC PARAMETERS

Model atmospheres were calculated using the ATLAS 12 code. The VALD atomic line database (Kupka et al. 1999), which also contains Kurucz (1993) data, was used to create a line list for the synthetic spectra. The SYNSPEC code (Hubeny, Lanz & Jeffery 1994, Krtićka 1998) was used to generate synthetic spectra adopting a microturbulence of 2 km s^{-1} . The computed spectra were convolved with the instrumental profile (a Gaussian of 0.2 Å FWHM for the Coudé spectra and 1.5 Å FWHM for the WIRO spectra) and rotationally broadened to fit the observed spectrum.

The best fit for the $H\beta$ and $H\alpha$ lines was obtained for $T_{\text{eff}} = 6950 \pm 100\text{ K}$, $\log g = 3.7 \pm 0.1$. We used the Mg II λ 4481 Å line for the determination of projected rotational velocity. The match between the synthetic and observed profile resulted in $v \sin i = 50 \pm 10\text{ km s}^{-1}$. In Fig. 1 we show the best fit for $H\beta$ together with a fit using two other effective temperatures for comparison.

4 THE KEPLER PHOTOMETRY

Kepler data were used to derive the frequency content of KIC 6382916. The *Kepler* Mission, designed to detect Earth-like planets using the transit method (Koch et al. 2010), was launched on 2009 March 6. *Kepler* has observed, and is continuing to observe, about 150 000 stars in a fixed field of view. The superb photometric precision and the almost continuous data coverage is of great advantage in determining the pulsational frequencies which can then be used to fit the ground-based data. *Kepler* observations consist mostly of long-cadence (LC) exposures of 30-min duration, but a few thousand stars, including KIC 6382916, were observed using 1-min (short cadence, SC) exposures.

The LC data are of limited value since the maximum

Table 1. Modes of highest amplitude in KIC 6382916 extracted from *Kepler* photometry. The first column is the name of the mode. The frequencies f (d^{-1}), amplitudes A (mag) and phases ϕ (radians) and the signal-to-noise ratio are listed. The standard deviation in the last digits is given. The epoch of phase zero is BJD 2454833.00.

Name	f (d^{-1})	A (mag)	ϕ	S/N
f_1	4.910722(8)	0.08067(3)	0.26626(6)	1406
f_2	6.431366(9)	0.07852(3)	0.39624(7)	1107
f_3	8.035055(54)	0.01233(3)	0.58971(42)	158
f_4 ($f_1 + f_2$)	11.342088(22)	0.03077(3)	0.61926(17)	325
f_5 ($2f_1$)	9.819598(39)	0.01734(3)	0.93893(30)	209
f_6 ($f_2 - f_1$)	1.522490(34)	0.01624(3)	0.92359(27)	250
f_7 ($2f_2$)	12.863552(50)	0.01337(3)	0.23045(39)	144

frequency that can be extracted is about 24 d^{-1} . We therefore used only the SC data which consists of 38314 points between JD 2455064.38 and JD 2455091.48 (27.1 d) taken at *Kepler* quarter 2.3 (Q2.3). With SC data frequencies as high as 700 d^{-1} can be detected if they are present. The data were prepared for analysis by cotrending and detrending the Simple Aperture Photometry (SAP) fluxes. The cotrending process was applied to the Q2.3 data using Cotrending Basis Vector (CBV) files which help to remove instrumental systematics from the light curve (Fraquelli & Thompson 2012; Christiansen et al. 2012). **KEPCOTREND**¹ package that is provided by NASA Kepler Science Center is used during cotrending process. All data points were converted to magnitudes (m_i) using the formula $m_i = -2.5 \log F_i$, where F_i is the raw SAP flux. A linear trend to m_i as a function of time was removed so that the final magnitudes have zero mean.

We used **PERIOD04** (Lenz & Breger 2005) to perform the frequency extraction. Frequencies were extracted by successive prewhitening until the signal-to-noise threshold $S/N = 3.5$ was reached. All peaks with S/N greater than this value were deemed significant (Breger et al. 2011). We found that the light curve can be described by two independent frequencies, $f_1 = 4.9107$ and $f_2 = 6.4314 \text{ d}^{-1}$, together with their harmonics and a few hundred combination terms. A third independent frequency, $f_3 = 8.0350 \text{ d}^{-1}$, is also present but has a much lower amplitude. The amplitude spectrum is shown in Fig. 2. Apart from f_1 and f_2 , the peaks of highest amplitude are the combination terms $f_1 + f_2$ and $f_2 - f_1$ and the harmonics $2f_1, 2f_2$. The lowest frequency that appears significant is $f_2 - f_1 = 1.520 \text{ d}^{-1}$. For the calculation of phase differences and amplitude ratios at different wavebands, we only considered the first seven frequencies of highest amplitude. These frequencies and their amplitudes and phases are listed in Table 1.

5 GROUND-BASED PHOTOMETRY

Photometric observations of KIC 6382916 were obtained at five different observatories located in North America and Europe. A total of 288 hours of observation was accumulated over 53 nights within the 85-d duration of the campaign. The campaign began in 2011 June and ended in 2011

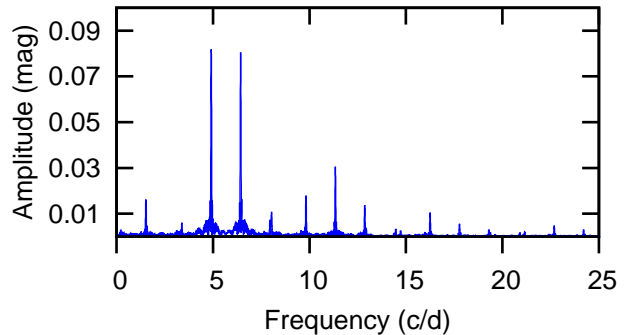


Figure 2. Fourier spectrum of KIC 6382916 for SC *Kepler* data

Table 2. Information on the photometric multi-site campaign. BNAO-Rozhen: Bulgarian National Astronomical Observatory-Rozhen; OAVdA: The Astronomical Observatory of the Autonomous Region of the Aosta Valley; SPM: Observatorio de San Pedro Mártir; RBO: Red Butte Observatory; CrAO: Crimean Astrophysical Observatory. The telescope apertures are in m. The total number of nights observed and the start end ending Julian dates of the observations relative to JD 24455000 are given.

Obs.	Site	Tel.	CCD-PMT
BNAO-Rozhen	Bulgaria	0.60–0.70	FLI PL9000–16803
OAVdA	Italy	0.81	FLI PL3041-1-BB
SPM	Mexico	0.84	FLI Fairchild F3041
RBO	USA	0.60	Apogee Alta E47-UV
CrAO	Ukraine	1.25	FLI PL1001E-1
CrAO	Ukraine	1.25	5-channel UBVR photometer-polarimeter

Obs.	Filters	Dates	Nights
BNAO-Rozhen	BVRI	3	735.35–782.56
OAVdA	BVRI	17	740.38–782.62
SPM	UBVR _c I _c	14	724.74–802.67
RBO	UBVRI	6	767.71–791.96
CrAO	UBVR _c I _c	13	719.29–804.48

September (JD 2455719.29–2455804.48). All data were obtained with either CCD or PMT detectors attached to five different telescopes in the UBVR photometric bands. A detailed description of the observations is given in Table 2.

The PMT data were only obtained using the 1.25-m telescope equipped with a five-channel photometer/polarimeter at CrAO. Since no U filter was available at BNAO-Rozhen and OAVdA, CCD measurements were ob-

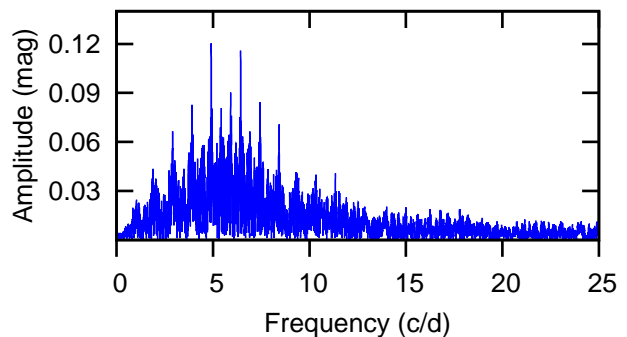


Figure 3. Fourier spectrum of ground-based data before prewhitening

¹ <http://keplergo.arc.nasa.gov/ContributedSoftwareKepcotrend.shtml>

tained only in *BVRI*. Furthermore, the *U* data from WIRO and CrAO suffers from instabilities due to the poor quality of the data. As a result, the frequencies in the *U* band could not be properly resolved and therefore we decided to omit the *U* observations for the purpose of mode identification. All the data sets from different sites were checked carefully and prepared for Fourier analysis by removing outliers caused by bad weather conditions or some other reason. The *R* and *I* filters are all of the Johnson/Bessel type except for SPM (Mexico) and CrAO (Ukraine) which are of the Cousins/Kron type. These filter differences have a negligible effect on the resulting amplitude ratios and the phase differences and no specific correction was applied.

Data reduction was performed by following the standard procedures. For the CCD observations, the data were reduced with standard **IRAF** routines including dark frame, bias subtraction and flat-field corrections for each CCD frame. Data taken with the different instruments were reduced with respect to only one comparison star, GSC 3144 0053, which could be observed in the CCD field at all sites. Instrumental magnitudes were obtained with the **DAOPHOT II** package (Stetson 1987) for aperture photometry. The PMT data from CrAO were reduced by following the traditional steps of obtaining differential magnitudes, sky subtraction and differential atmospheric extinction corrections using the same comparison star. Finally, the times were converted to Heliocentric Julian Date (HJD).

Since the telescopes and instruments used at the observing stations were not exactly the same, measurements from different sites have different zero points. In order to determine the zero point differences in each filter for each site, we assume that the light curve is well represented by a truncated Fourier series using frequencies derived from the *Kepler* photometry (Ulusoy et al. 2013). The Fourier spectrum of the data before prewhitening can be seen in Fig. 3. Using the first seven frequencies of highest amplitude extracted from the SC *Kepler* data, the individual zero points for the different sites together with the number of observations are shown in Table 3. The amplitudes and phases were determined by least-square fitting with the three independent frequencies: $f_1 = 4.9107$, $f_2 = 6.4314$ and $f_3 = 8.0350 \text{ d}^{-1}$, the harmonics of f_1 and f_2 ($2f_1$, $2f_2$) and the combination frequencies listed in Table. 4. The uncertainties were calculated as the standard deviations of each fitted parameter. The observed light variation of the star in the *V* filter together with the fitted Fourier series are shown in Fig. 4.

6 MODE IDENTIFICATION

Photometric mode identification is based on a comparison of observed amplitude ratios or phase differences with the computed values at different wavelengths. These differences are small and requires photometry of high accuracy. The best results are obtained with pulsations of high amplitude since the relative errors are smaller. With this in mind, we only considered the three independent modes with highest amplitudes in KIC 6382916. The method followed here is described in a previous multi-site campaign reported by Ulusoy et al. (2013). In order to calculate the amplitude ratios and phase differences in the Johnson/Cousins *BVRI* system for a given spherical harmonic degree, l , we made use of the **FAMIAS** soft-

Table 3. Zero points in the UBVRI filters for various sites and the number of observations, N .

Site	<i>U</i>	<i>N</i>		
Mexico	-2.863 ± 0.001	1395		
Site	<i>B</i>	<i>N</i>	<i>V</i>	<i>N</i>
Bulgaria	-1.446 ± 0.002	373	-0.276 ± 0.001	379
Italy	-1.118 ± 0.001	3474	-0.237 ± 0.001	3209
Mexico	-1.289 ± 0.001	1435	-0.288 ± 0.001	2814
Ukraine	-1.255 ± 0.001	11795	-0.213 ± 0.001	9985
USA	-1.211 ± 0.002	278	-0.267 ± 0.002	275
Site	<i>R</i>	<i>N</i>	<i>I</i>	<i>N</i>
Bulgaria	0.312 ± 0.001	372	0.919 ± 0.001	372
Italy	0.389 ± 0.001	2922	0.966 ± 0.001	2618
Mexico	0.317 ± 0.001	1420	0.942 ± 0.001	1390
Ukraine	0.395 ± 0.001	10587	1.039 ± 0.001	9423
USA	0.361 ± 0.002	273	0.987 ± 0.001	255

Table 4. Amplitudes, A (mag), and phases (radians) for the three frequencies of highest amplitude: $f_1 = 4.9107$, $f_2 = 6.4314$ and $f_3 = 8.0350 \text{ d}^{-1}$, their harmonics and linear combinations of f_1 and f_2 . The epoch of phase zero is JD 2455700.000.

ID	A_B	ϕ_B
f_1	0.1281 ± 0.0005	0.2668 ± 0.0006
f_2	0.1263 ± 0.0005	0.1294 ± 0.0006
f_3	0.0145 ± 0.0005	0.4718 ± 0.0056
$f_1 + f_2$	0.0469 ± 0.0005	0.1292 ± 0.0017
$2f_1$	0.0186 ± 0.0005	0.3068 ± 0.0043
$f_2 - f_1$	0.0139 ± 0.0005	0.2081 ± 0.0056
$2f_2$	0.0226 ± 0.0005	-0.3858 ± 0.0036
ID	A_V	ϕ_V
f_1	0.0929 ± 0.0003	0.2779 ± 0.0006
f_2	0.0925 ± 0.0003	0.1228 ± 0.0006
f_3	0.0141 ± 0.0003	-0.4650 ± 0.0037
$f_1 + f_2$	0.0335 ± 0.0003	0.1219 ± 0.0015
$2f_1$	0.0158 ± 0.0003	0.3565 ± 0.0033
$f_2 - f_1$	0.0150 ± 0.0003	0.2216 ± 0.0033
$2f_2$	0.0144 ± 0.0003	-0.3996 ± 0.0036
ID	A_R	ϕ_R
f_1	0.0696 ± 0.0003	0.2675 ± 0.0006
f_2	0.0683 ± 0.0003	0.1157 ± 0.0006
f_3	0.0109 ± 0.0003	-0.4611 ± 0.0041
$f_1 + f_2$	0.0234 ± 0.0003	0.1134 ± 0.0019
$2f_1$	0.0123 ± 0.0003	0.3460 ± 0.0036
$f_2 - f_1$	0.0086 ± 0.0003	0.1979 ± 0.0050
$2f_2$	0.0118 ± 0.0003	-0.4180 ± 0.0038
ID	A_I	ϕ_I
f_1	0.0487 ± 0.0003	0.2578 ± 0.0009
f_2	0.0488 ± 0.0003	0.1115 ± 0.0009
f_3	0.0089 ± 0.0003	-0.4289 ± 0.0048
$f_1 + f_2$	0.0169 ± 0.0003	0.1091 ± 0.0025
$2f_1$	0.0089 ± 0.0003	0.3375 ± 0.0047
$f_2 - f_1$	0.0040 ± 0.0003	0.1372 ± 0.0105
$2f_2$	0.0082 ± 0.0003	-0.3968 ± 0.0052

ware package (Zima 2008). This program uses pre-computed grids of non-adiabatic stellar models. The calculations need to be restricted to models in the appropriate range of T_{eff} , $\log g$, stellar mass and metallicity.

For KIC 6382916, we computed the amplitude ratios and phase differences in the *BVRI* bands for spherical harmonic degrees $0 \leq l \leq 3$. We adopted the stellar parameters

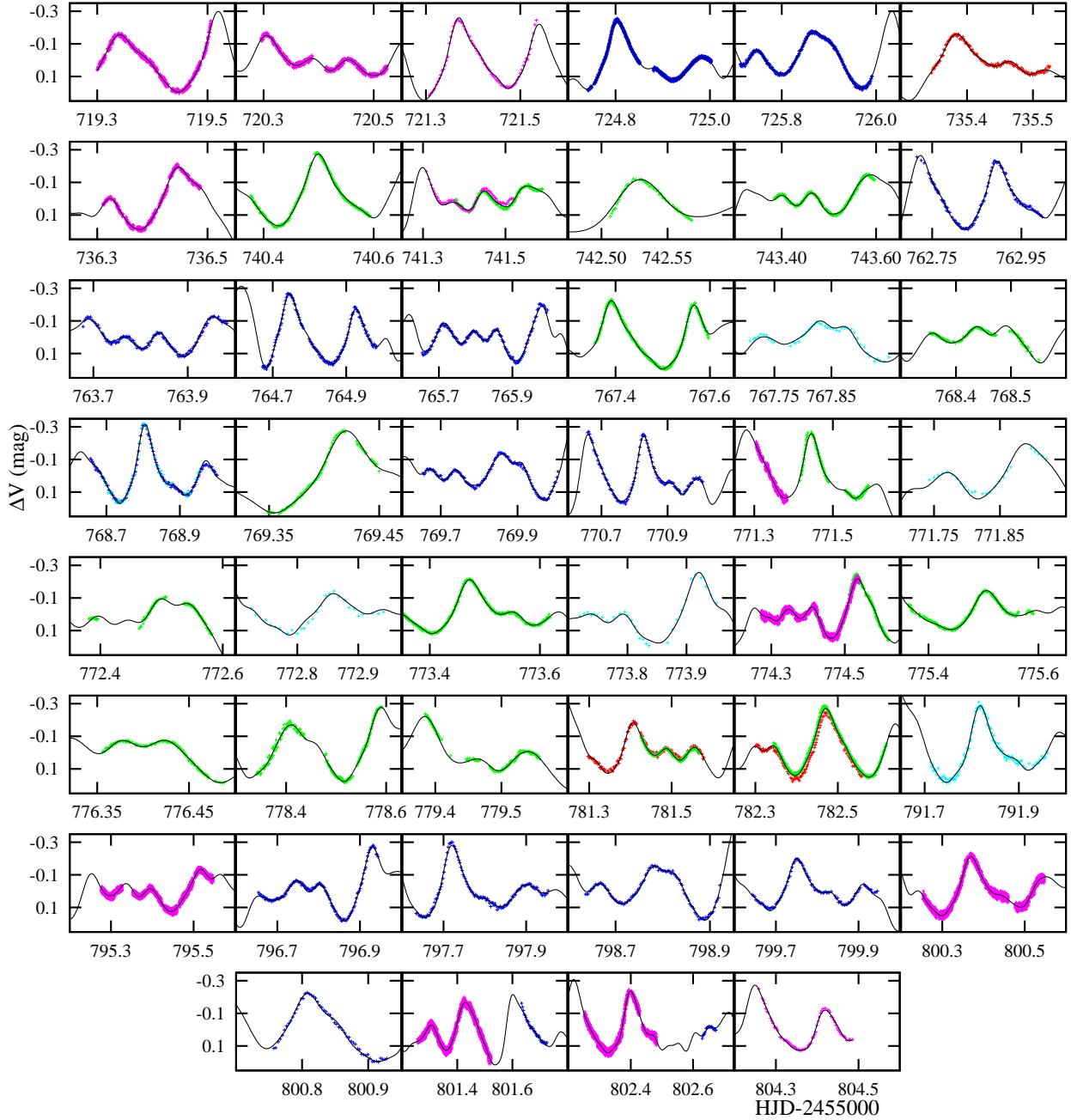


Figure 4. V filter light curves corrected for zero points showing fitted Fourier curve.

$T_{\text{eff}} = 6950 \pm 100$ K, $\log g = 3.7 \pm 0.1$ and microturbulent velocity $\xi = 2$ km s $^{-1}$. Using these parameters, the mass of KIC 6382916 is estimated to be $M = 1.93 \pm 0.27 M_{\odot}$ from the empirical relations in Torres et al. (2010). The amplitude ratios and phase differences depend on the stellar parameters. Since the estimated stellar parameters are not very precise, we decided to calculate these values over the range $6800 < T_{\text{eff}} < 7200$ K and $3.5 < \log g < 3.9$.

In FAMIAS, theoretical calculations are performed adopting a grid for δ Scuti stars computed with the ATON (Ventura et al. 2008) and MAD (Montalbán & Dupret 2007) codes. The uncertainty in the theoretical prediction of the amplitude ratios comes from the uncertainties of the pa-

rameters, amplitude, phase, effective temperature and $\log g$ (Zima 2008). The observed amplitude ratios and phase differences for f_1 , f_2 and f_3 normalized to the B filter are listed in Table 5. Comparison with the calculated values are shown in Fig. 5. Also, the relationship between the amplitude ratios, phases and these frequencies are shown in Fig. 6.

As can be seen from Fig. 5, the observed amplitude ratios for f_1 and f_2 agree quite well if $l = 1$ for both modes. We could not obtain a reliable mode identification for f_3 because of its low amplitude, but it appears to be either $l = 0$ or $l = 2$. The phase differences f_1 agree quite well for $l = 1$, though for f_2 they are intermediate between $l = 1$ and

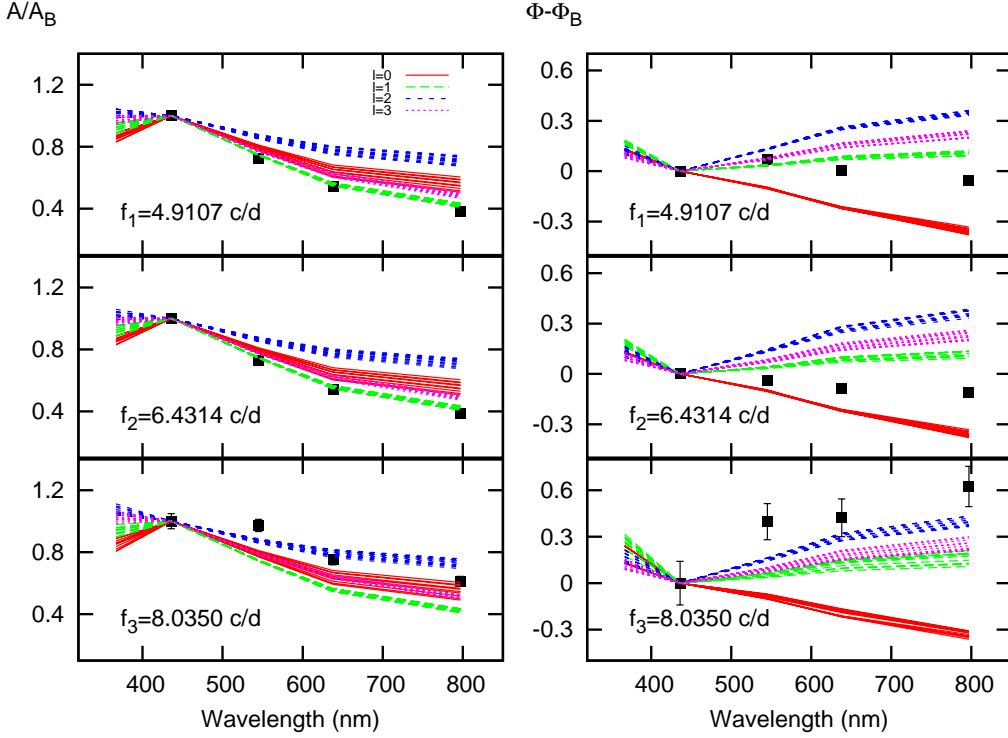


Figure 5. Amplitude ratios (left panels) and phase differences (radians, right panels) for f_1 , f_2 and f_3 . The curves are from models with a range of stellar parameters of the best estimated values with a range of stellar parameters of $6800 < T_{\text{eff}} < 7200$ K and $3.5 < \log g < 3.9$, and for different spherical harmonic degrees, l ($0 \leq l \leq 3$). The red (solid) lines indicate $l = 0$, the green (long-dashed) $l = 1$, the dark blue (dashed) $l = 2$ the purple (dotted) $l = 3$. The models computed for $M = 1.90M_{\odot}$. The black squares represent the observed values with their standard deviations for f_1 , f_2 and f_3 .

Table 5. Amplitude ratios, A/A_B , and phase differences, $\phi - \phi_B$, (radians) for the seven frequencies of highest amplitude.

Filters	A/A_B	$\phi - \phi_B$
f_1		
B	1.0000 ± 0.0055	0.0000 ± 0.0151
V	0.7252 ± 0.0037	0.0697 ± 0.0151
R	0.5433 ± 0.0031	0.0044 ± 0.0151
I	0.3802 ± 0.0028	-0.0565 ± 0.0188
$2f_1$		
B	1.0000 ± 0.0380	0.0000 ± 0.1081
V	0.8495 ± 0.0280	0.3123 ± 0.0955
R	0.6613 ± 0.0240	0.2463 ± 0.0993
I	0.4785 ± 0.0206	0.1929 ± 0.1131
f_2		
B	1.0000 ± 0.0056	0.0000 ± 0.0151
V	0.7324 ± 0.0037	-0.0415 ± 0.0151
R	0.5408 ± 0.0032	-0.0861 ± 0.0151
I	0.3864 ± 0.0028	-0.1125 ± 0.0188
$2f_2$		
B	1.0000 ± 0.0313	0.0000 ± 0.0905
V	0.6372 ± 0.0194	-0.0867 ± 0.0905
R	0.5221 ± 0.0176	-0.2023 ± 0.0930
I	0.3628 ± 0.0155	-0.0691 ± 0.1106
f_3		
B	1.0000 ± 0.0488	0.0000 ± 0.1407
V	0.9724 ± 0.0394	0.3971 ± 0.1169
R	0.7517 ± 0.0332	0.4216 ± 0.1219
I	0.6138 ± 0.0296	0.6239 ± 0.1307

$l = 0$. Overall, it seems as if f_1 and f_2 are both dipole modes. The radial mode seems to be ruled out for both modes.

7 CONCLUSIONS

Analysis of short-cadence *Kepler* photometry was used to determine the pulsation frequencies in KIC 6382916. We find two large-amplitude independent modes with frequencies $f_1 = 4.9107$ and $f_2 = 6.43137 \text{ d}^{-1}$ as previously reported by Pigulski et al. (2009) from ground-based observations. We found a third independent frequency at $f_3 = 8.03506 \text{ d}^{-1}$ which has a much lower amplitude. The frequency spectrum is dominated by f_1 and f_2 and their harmonics and combination frequencies.

In HADS stars the modes of highest amplitude are generally radial modes since in many stars the period ratio P_1/P_0 of first overtone to fundamental radial modes is close to the expected value $0.77 < P_1/P_0 < 0.78$. The stars lie on a curve defined by P_1/P_0 as a function of $\log P_0$ which is called the Petersen diagram (Petersen 1973). The period ratio depends on metallicity, rotation and chemical abundance (Lenz et al. 2008; Suárez et al. 2007). In KIC 6382916 the period ratio for the two modes of highest amplitude is $f_1/f_2 = 0.763$ which differs significantly from the expected period ratio for fundamental and first overtone radial modes. It therefore seems that at least one of the two modes is probably a nonradial mode. This may not be too surprising since recent studies suggest that the radial mode need not be present in all HADS stars (Poretti et al. 2011).

To determine the spherical harmonic degree of the three independent modes in KIC 6382916 we first of all need to know the stellar parameters as accurately as possible. For this purpose we obtained high-dispersion spectra and esti-

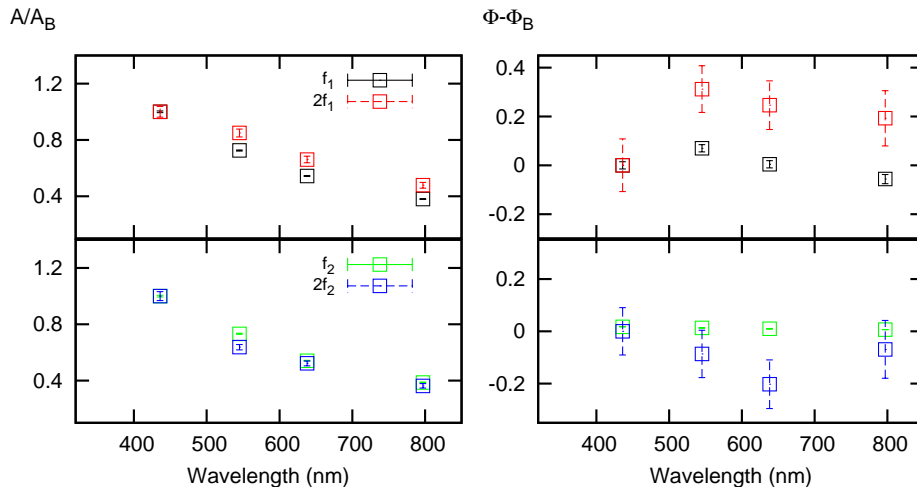


Figure 6. Amplitude ratios (left panel) and phase differences (radians, right panel) for f_1 , f_2 and its harmonics, $2f_1$, $2f_2$.

mated an effective temperature $T_{\text{eff}} = 6950 \pm 100$ K and $\log g = 3.7 \pm 0.1$ by matching the Balmer line profiles with profiles calculated from synthetic spectra. From the effective temperature and surface gravity we estimate the mass as $M = 1.93 \pm 0.27 M_{\odot}$.

Mode identification is best done by comparing the relative amplitude ratios and/or phase differences in different photometric wavebands for the required mode with the calculated values. For this purpose we initiated a multi-site photometric campaign to observe KIC 6382916 in the *BVRI* bands. We used the frequencies derived from the *Kepler* data as fixed values and fitted a truncated Fourier series to the data from each wave band using the seven frequencies of highest amplitude. The resulting amplitude and phases were used to construct the relative amplitudes and phase differences, normalized to the *B* band, for f_1 , f_2 and f_3 . We then used the *FAMIAS* software package (Zima 2008) to calculate amplitude ratios and phase differences for models with stellar parameters approximately corresponding to the spectroscopic values mentioned above. It turns out that f_1 and f_2 are both dipole ($l = 1$) modes and that f_3 is either $l = 0$ or $l = 2$.

If the identification for both f_1 and f_2 is correct, it calls to mind the case of 1 Mon (Balona & Stobie 1980; Balona et al. 2001). In this star there are three modes: a central radial mode flanked by two $l = 1$ modes. In any case it seems that we need to be cautious in attributing the high-amplitude modes in HADS stars as radial modes, though this is probably true in the majority of cases.

It is important to compare the observed frequencies of f_1 and f_2 with model frequencies for $l = 1$. However, we are faced with the problem that rotation strongly modifies the frequencies of the $l = 1$ modes. We therefore need to estimate the possible frequency shift owing to this effect which requires knowledge of the rotation frequency. In some δ Sct stars, it is possible to detect the rotational frequency directly from the periodogram of the *Kepler* data by looking for the presence of a low-frequency peak and its harmonic. The presence of an harmonic is an indicator that the peak is due to a starspot and hence the frequency is the rotational frequency (Balona 2013). Unfortunately, no such peak is visible in KIC 6382916.

The alternative is to estimate the rotational frequency from the projected rotational velocity $v \sin i = 50 \pm 10 \text{ km s}^{-1}$ and the stellar radius. The stellar radius is estimated to be about $3.69 \pm 0.14 R_{\odot}$ using the relationships by Torres et al. (2010). If we assume that the star is roughly equator-on, the equatorial rotational velocity will probably be about 50 km s^{-1} and the rotation frequency around 0.27 d^{-1} . If the star is equator-on, only sectorial modes will be visible and the frequency shift will roughly be the same as the rotation frequency. Thus we may expect the frequencies in the non-rotating frame to be in the range $4.6 < f_1 < 5.2$ and $6.1 < f_2 < 6.7$.

We can compare these frequencies with frequencies calculated from non-rotating models. For this purpose, models of δ Scuti stars with masses in the range $1.3 < M/M_{\odot} < 2.5$ were constructed using the Warsaw - New Jersey code (Paczynski 1970). These models use OPAL opacities, no core overshoot and a mixing length, $\alpha = 1.0$. Pulsation frequencies for each model were obtained using the NADROT code (Dziembowski 1977). It turns out that all modes with frequencies less than about 6.1 d^{-1} are stable. One may argue that the rotation frequency is much larger and that the rotation correction would then bring f_1 closer to this value. This argument cannot be correct since this would imply a nearly pole-on orientation, in which case sectorial modes are no longer visible. We are thus faced with the problem that current models are unable to account for driving at the low frequency of f_1 . Models where f_1 and f_2 are both present (but with f_1 stable) all have $6800 < T_{\text{eff}} < 7200$ K and $3.78 < \log g < 3.88$ which is roughly in the range of the values determined from spectroscopy. In the model, frequencies in the range of f_1 and f_2 are mixed p and g modes of high radial order, but this does not mean that the observed modes are also of this kind since no model is capable of driving these frequencies. The lowest frequency of a p mode for models in the above parameter range is about 8.6 d^{-1} . They all appear to be g modes of high order. The lowest frequency of a p mode for models in the above parameter range is about 8.6 d^{-1} .

In conclusion, we find that the two modes of highest amplitude in KIC 6382916 are not only dipole modes, contrary to expectation, but are high-order g modes which are pre-

dicted to be stable in the models. Unless the derived stellar parameters are grossly in error, this would imply a problem in our understanding of pulsational driving in δ Scuti stars. We know that there is a problem with the models in that the observed range of instability is wider than the calculated range for δ Sct stars (Balona & Dziembowski 2011). It appears that the presence of two high-amplitude g modes in KIC 6382916 is further confirmation of this problem.

ACKNOWLEDGMENTS

The authors acknowledge the whole *Kepler* team for providing the unprecedented data sets that makes these results possible. This paper includes data collected by the *Kepler* mission. Funding for the *Kepler* mission is provided by the NASA Science Mission directorate. CU sincerely thanks the South African National Research Foundation (NRF) for the award of innovation post doctoral fellowship, Grant No. 73446. BU is supported by the project numbered HDYF-051. TG would like to thank NRF Equipment-Related Mobility Grant-2011 for travelling to carry out the photometric observations. LAB thanks the South African National Research Foundation and the South African Astronomical Observatory for generous financial support. IS and II gratefully acknowledge the partial support from Bulgarian NSF under grant DO 02-85. DD acknowledges for the support of grants DO 02-362 and DDVU 02/40-2010 of Bulgarian NSF. HAK acknowledges Carlos Vargas-Alvarez, Michael J. Lundquist, Garrett Long, Jessie C. Runnoe, Earl S. Wood, Michael J. Alexander for helping with the observations at WIRO. LFM acknowledges financial support from the UNAM under grant PAPIIT 104612 and from CONACYT by the way of grant 118611. MD, AC and DC are supported by grants provided by the European Union, the Autonomous Region of the Aosta Valley and the Italian Department for Work, Health and Pensions. The OAVdA is supported by the Regional Government of the Aosta Valley, the Town Municipality of Nus and the Mont Emilius Community. TEP acknowledges support from the National Research Foundation of South Africa. This study made use of IRAF Data Reduction and Analysis System and the Vienna Atomic Line Data Base (VALD) services. The authors thank Dr Zima for providing the FAMIAS code.

REFERENCES

- Balona L. A., Stobie R. S., 1980, MNRAS, 190, 931
 Balona L. A., et al., 2001, MNRAS, 321, 239
 Balona L. A., Dziembowski W. A., 2011, MNRAS, 417, 591
 Balona, L.A. et al., 2012, MNRAS, 419, 3028
 Balona L. A., 2013, MNRAS, 1036
 Breger, M., Pamyatnykh, A. A., 1998, A&A, 332, 958
 Breger M., 2000, Balt. Astron., 9, 149
 Breger M. et al., 2011, MNRAS, 414, 1721
 Christiansen, J. L. et al. 2012, Kepler Data Release 14 Notes (KSCI-19054-001)
 Dziembowski W., 1977, Acta Astron., 27, 95
 Fraquelli, D., Thompson, S. E., 2012, Kepler Archive Manual (KDMC-10008-004)
 Gilliland R. L. et al., 2010, ApJ, 713, L160
 Hubeny I., Lanz T., Jeffery C.S., 1994, in Jeffery C.S., ed, Newsletter on Analysis of Astronomical spectra, No.20, CCP7. St. Andrews Univ., St.Andrews, p. 30
 Jenkins J. M. et al., 2010, ApJ, 713, L120
 Koch, D. G. et al., 2010, ApJ, 713, 79
 Krtićka J., 1998, in Dušek J., Zejda M., eds, Proc. 20-th Stellar Conf. Nicholas Copernicus Observatory and Planetarium, Brno, p. 73
 Kupka F. et al., 1999, A&AS, 138, 119
 Kurucz R.L., 1993, SYNTHE spectrum synthesis programs and line data (Kurucz CD-ROM 18)
 Lenz, P., Breger, M., 2005, Commun. Asteroseismol. 146, 53
 Lenz, P. et al., 2008, A&A, 478, 855
 McNamara, D.H. 2000, in Delta Scuti and Related Stars, M. Breger and M.H. Montgomery Eds., ASP Conf. Series, 210, 373
 Montalbán, J., Dupret, M. A., 2007, A&A, 470, 991
 Paczynski B., 1970, Acta Astronomica, 20, 47
 Petersen, J. O., 1973, A&A, 27, 89
 Pigulski, A. et al., 2009, Acta Astronomica, 59, 33
 Poretti, E., 2003, A&A, 409, 1031
 Poretti et al., 2005, A&A, 440, 1097
 Poretti et al., 2011, A&A, 528, 147
 Reegen P., 2007, A&A, 467, 1353
 Soszynski I. et al., 2008, Acta Astronomica, 58, 163
 Stetson P. B., 1987, PASP, 99, 191
 Suárez, J. C. et al., 2007, A&A, 474, 961
 Torres G., Andersen J., Giménez A., 2010, A&ARv, 18, 67
 Ulusoy, C. et al., 2013, MNRAS, 428, 3551
 Ventura, P. et al., 2008, AP&SS, 316, 93
 Zima W., 2008, CoAst, 155, 17